Molecular Pharmacology Fast Forward. Published on September 6, 2018 as DOI: 10.1124/mol.118.113357
This article has not been copyedited and formatted. The final version may differ from this version.

Title Page

Activation of *Caenorhabditis elegans* levamisole-sensitive and mammalian nicotinic receptors by the antiparasitic bephenium

Ornella Turani, Guillermina Hernando, Jeremías Corradi, and Cecilia Bouzat

Instituto de Investigaciones Bioquímicas de Bahía Blanca (INIBIBB), Departamento de Biología, Bioquímica y Farmacia, Universidad Nacional del Sur-Consejo Nacional de Investigaciones Científicas y Técnicas (CONICET), Bahía Blanca, Argentina.

Molecular Pharmacology Fast Forward. Published on September 6, 2018 as DOI: 10.1124/mol.118.113357
This article has not been copyedited and formatted. The final version may differ from this version.

Abstract

Nicotinic acetylcholine receptors (nAChRs) are ligand-gated ion channels involved in neuromuscular transmission. In nematodes, muscle nAChRs are targets of antiparasitic drugs. Bephenium is an anthelmintic compound whose molecular action at the free-living nematode *Caenorhabditis elegans,* which is a model for anthelmintic drug discovery, is poorly known. We explored its effect on *C. elegans* locomotion and applied single-channel recordings to identify its molecular target, mechanism of action, and selectivity between mammalian and *C. elegans* nAChRs. As in parasites, bephenium paralyzes *C. elegans*. A mutant strain lacking the muscle levamisole-sensitive nAChR (L-AChR) shows full resistance to bephenium, indicating that this receptor is the target site. Bephenium activates L-AChR channels from larvae muscle cells in the micromolar range. Channel activity is similar to that elicited by levamisole, appearing mainly as isolated brief openings. Our analysis revealed that bephenium is an agonist of L-AChR and an open-channel blocker at higher concentrations. It also activates mammalian muscle nAChRs. Opening events are significantly briefer than those elicited by ACh and do not appear in activation episodes at a range of concentrations, indicating that it is a very weak agonist of mammalian nAChRs. Recordings in the presence of ACh showed that bephenium acts as a voltage-dependent channel blocker and a low-affinity agonist. Molecular docking into homology modeled binding-site interfaces proposed binding modes for bephenium that explain its partial agonism. Given the great diversity of helminth nAChRs and the overlap of their pharmacological profiles, unravelling drug selectivity basis is required for rational design of anthelmintic drugs.

Molecular Pharmacology Fast Forward. Published on September 6, 2018 as DOI: 10.1124/mol.118.113357
This article has not been copyedited and formatted. The final version may differ from this version.

Introduction

The prevalence of human and animal infections with helminths, commonly known as parasitic worms, remains staggeringly high, thus urging the need for concerted efforts on this area of research. Parasitic nematodes (roundworms) are not ideal laboratory animals because of the difficulty for genetic manipulation and the need for infected host animals. In this context, the free-living nematode *Caenorhabditis elegans* has emerged as a powerful model system for anthelmintic drug screening: It shares physiological and pharmacological characteristics with parasitic nematodes, it is no more dissimilar to parasitic nematodes than each individual species of parasite is to one another, and it is sensitive to most anthelmintic drugs (Holden-Dye and Walker, 2007).

Nicotinic receptors (nAChRs), which have a key role in muscle contraction and locomotion in vertebrates and invertebrates, are targets of anthelmintic agents. They belong to the Cys-loop receptor family of pentameric ligand-gated ion channels that contain a large extracellular domain that carries the agonist binding sites and a transmembrane domain that forms the ion channel (Unwin, 2005; Kalamida et al., 2007; Cecchini and Changeux, 2015; Bouzat and Mukhtasimova, 2018). The agonist binding sites are located at subunits interfaces, where one subunit contributes to the principal face and the adjacent one, to the complementary face. Only α-type subunits, which contain a conserved disulphide bridge in Loop C of the binding site, form the principal face of the binding site whereas the complementary face can be formed by either α or non-α subunits (Sine et al., 2012).

Vertebrates contain 17 nAChR subunits that yield a variety of receptors. The mammalian muscle nAChR is formed by four different subunits, α1, β1, δ and γ or ε depending if it is embryonic or adult muscle, respectively, with an $(\alpha1)_2\beta\delta\ \varepsilon/\gamma$ composition. The two agonist binding sites occur at α1/δ and α1/γ or ε subunit interfaces. *C. elegans* possesses an extensive gene family of nAChR subunits (Jones et al., 2007; Jones and Sattelle, 2008). At its neuromuscular junction, the two main nAChRs are the nicotine-sensitive (N-AChR) and the levamisole-sensitive (L-AChR) (Richmond and Jorgensen, 1999). The L-AChR is the target of nematocide agents, such as levamisole and pyrantel, which, by acting as potent agonists, produce body-wall muscle hypercontraction, paralysis, and ultimately death. It is composed of five different subunits, three of which are essential (UNC-63, UNC-38, and UNC-29) and the other two (LEV-8 and LEV-1) are non-essential (Boulin et al., 2008; Hernando et al., 2012). The disposition of the five subunits in the pentameric arrangement remains unknown. Null mutants of essential subunits show

Molecular Pharmacology Fast Forward. Published on September 6, 2018 as DOI: 10.1124/mol.118.113357
This article has not been copyedited and formatted. The final version may differ from this version.

uncoordinated phenotypes and resistance to anthelmintic agents whereas only partial resistance is observed in null mutants of non-essential subunits (Lewis et al., 1980). UNC-63, UNC-38 and LEV-8 are α-type subunits and can contribute to the principal face of the binding site. ACR-8, a muscle α-type subunit homologous to LEV-8 (Mongan et al., 1998), acts as a spare subunit for *C. elegans* L-AChR (Hernando et al., 2012).

Parasitic nematodes contain nAChR subunit genes that show high similarity with their *C. elegans* counterparts. Whereas *C. elegans* muscle contains two main nAChR subtypes (L- and N-) of fixed subunit composition, parasitic nematode muscle has a larger diversity of nAChRs due to subunit duplication and to different arrangements of the orthologous subunits (Qian et al., 2006; Boulin et al., 2008, 2011; Buxton et al., 2014; Duguet et al., 2016; Verma et al., 2017). In different species, L-, N-, P- (pyrantel), M- (morantel), and B- (bephenium) subtypes were described (Martin et al., 1997; Robertson et al., 2002; Qian et al., 2006; Verma et al., 2017).

Bephenium is an anthelmintic compound used against human and dog hookworms and gastrointestinal parasitic nematodes in sheep (Burrows, 1958; Copp et al., 1958; Young et al., 1958). Unlike levamisole and pyrantel, the activity of bephenium on the parasite model *C. elegans* as well as its mechanism and target sites are poorly known. We here revealed the effect of this drug on *C. elegans* locomotion and we identified its molecular target, mechanism of action, structural basis of action, and differences in activation between mammals and *C. elegans*.

Molecular Pharmacology Fast Forward. Published on September 6, 2018 as DOI: 10.1124/mol.118.113357
This article has not been copyedited and formatted. The final version may differ from this version.

Materials and Methods

Drugs.

Acetylcholine chloride, levamisole hydrochloride and bephenium hydroxynaphthoate were from Sigma-Aldrich (Merck, KGaA, Darmstadt, German).

Caenorhabditis elegans strains and culture.

Nematode strains used were: N2 Bristol wild-type; PD4251: *ccIs4251*;*dpy-20*(*e1282*) which produces green fluorescence protein (GFP) in all body wall muscles and vulval muscles; ZZ15: *lev-8*(*x15*) a *lev-8* null mutant strain with partial resistance to levamisole; CB904: *unc-38(e264)I* which lacks UNC-38 essential subunit that integrates L-AChR. All nematodes strains were obtained from the *Caenorhabditis* Genetic Center, which is funded by the NIH National Center for Research Resources (NCRR). Nematode strains were maintained at 18–25°C using freshly prepared Nematode Growth Medium (NGM) petri dishes that have been spread with *Escherichia coli* (OP50) as a source of food (Rayes et al., 2007; Hernando, et al., 2012).

Isolation and culture of C. elegans embryonic muscle cells.

Embryonic cells were isolated and cultured as previously described (Christensen et al., 2002; Rayes et al., 2007). Briefly, adult nematodes were exposed to an alkaline hypochlorite solution (0.5 M NaOH and 1 % NaOCl) and the eggs released were treated with 1.5 units/ml chitinase (Sigma-Aldrich Co., St. Louis, MO) for 30-40 min at room temperature. The embryo cells were isolated by gently pipetting and filtering through a sterile 5-µm Durapore syringe filter (Millipore Corp., Bedford, MA) to remove undissociated embryos and newly hatched larvae. Filtered cells were plated on glass coverlips coated with poly-O-Ornithine. Cultures were maintained at 24 °C in a humidified incubator in L-15 medium (Hyclone, Logan, UT) containing 10 % fetal bovine serum. Complete differentiation to the various cell types that comprise the newly hatched L1 larva were observed within 24 h. Electrophysiological recordings were performed 1-5 days after cell isolation. Muscle cells are easily identifiable due to their spindle-shaped morphology, which resembles that of body wall muscle cells in vivo (Christensen et al., 2002; Rayes et al., 2007; Hernando et al., 2012).

Isolation and culture of C. elegans L2 muscle cells.

Molecular Pharmacology Fast Forward. Published on September 6, 2018 as DOI: 10.1124/mol.118.113357
This article has not been copyedited and formatted. The final version may differ from this version.

Adult nematodes were exposed to an alkaline hypochlorite solution (0.5 M NaOH and 1 % NaOCl) and the eggs released were grown in petri dishes spread with dead *Escherichia coli* (OP50) to avoid cell culture contamination. Synchronized L2 larvae were used for cells isolation in sterile conditions. The worms were exposed to a SDS (sodium dodecyl sulfate)-DTT (dithiothreitol) solution to weaken the cuticle. Then, the pronase E enzyme was added to disrupt the cuticle and release live cells from larval worms. When combined with mechanical disruption by pipetting, pronase and SDS-DTT treatment dissociate tissues and release single cells very efficiently. Filtered cells were plated on glass coverslips and maintain in culture like the embryonic muscle cells (Zhang et al., 2011; Zhang and Kuhn, 2012; Spencer et al., 2014). Electrophysiological recordings were performed 1-5 days after cell isolation.

Paralysis assays.

Drug sensitivity was determined by paralysis assays on agar plates with young adult hermaphrodite worms from synchronized plates. Worms (about 30-50 animals) were placed on agar plates containing the tested drug at room temperature as described before (Hernando et al., 2012). Body paralysis was defined as the lack of complete body movement in response to prodding. The paralysis was evaluated under magnifying glass at the indicated time (every 30–60 minutes).

Mammalian cell expression of muscle nAChR.

BOSC cells (derived from HEK 293 cells, Pear et al., 1993) were transfected with mouse adult muscle nAChR subunit cDNAs using calcium phosphate precipitation, as described previously (Bouzat et al., 1994; Bouzat et al., 2000). The subunit cDNA ratio was 2α1:1β:1ε:1δ, with a total cDNA amount of 5 μg/ 35 mm dish. A plasmid encoding green fluorescent protein was also included to allow identification of transfected cells under fluorescence optics. Cells were used for single-channel measurements 2 days after transfection.

Patch-clamp recordings.

Single-channel currents were recorded in the cell-attached patch configuration at 20°C (Rayes et al., 2007; Hernando et al., 2012). The bath and pipette solutions contained 140 mM KCl, 5.4 mM NaCl, 1.8 mM $CaCl_2$, 1.7 mM $MgCl_2$, and 10 mM HEPES (pH 7.4). The stock solution for bephenium was prepared in dimethyl sulphoxide (DMSO) and the final

Molecular Pharmacology Fast Forward. Published on September 6, 2018 as DOI: 10.1124/mol.118.113357
This article has not been copyedited and formatted. The final version may differ from this version.

DMSO concentration used in all assays was lower than 0.1%. Single-channel currents were recorded using an Axopatch 200 B patch-clamp amplifier (Molecular Devices, Inc., Sunnyvale, CA), digitized at 10 μs intervals with the PCI 6111E interface (National Instruments, Austin, TX), recorded using the program Acquire (HEKA Instruments Inc., Bellmore, NY) and detected by the half-amplitude threshold criterion using the TAC 4.0.10 program (Bruxton Corporation, Seattle, WA) at a final bandwidth of 9 kHz. Open- and closed-time histograms were plotted using a logarithmic abscissa and a square root ordinate and fitted to the sum of exponential functions by maximum likelihood using the program TACFit (Bruxton Corporation). Clusters of channel openings were identified as a series of closely separated openings preceded and followed by closings longer than a critical duration (τ_{crit}). This duration was taken as the point of intersection of the predominant closed component and the succeeding one (longer duration) in the closed time histogram (Bouzat et al., 2000; Corradi et al., 2009). For the mammalian nAChR, τ_{crit} was defined by the point between the main closed component, which is sensitive to ACh concentration, and the previous one (typically 10-16 ms for 30 μM ACh at -70 mV membrane potential). Cluster durations were determined from the longest duration component of open time histograms with τ_{crit} set to the corresponding value, and therefore openings separated by closing briefer than this time constitute a cluster.

Macroscopic currents were recorded in the whole-cell configuration as described before (Gumilar et al., 2003). Briefly, the pipette solution contained 134 mM KCl, 5 mM EGTA, 1 mM MgCl2, and 10 mM HEPES (pH 7.3). The extracellular solution (ECS) contained 150 mM NaCl, 0.5 mM CaCl2, 10 mM HEPES (pH 7.4). 1.5-s pulses of ECS containing ACh or bephenium were applied. The solution exchange time was estimated by the open pipette and varied between 0.1 and 1 ms.

Molecular modeling and docking.

Homology models of the extracellular domain of two adjacent subunits were created using the structure of the human α4β2 nicotinic receptor in complex with nicotine (Protein Data Bank code 5KXI, Morales et al., 2016) and the chimera α7/AChBP (Acetylcholine binding protein) crystalized with the partial agonist lobeline that contains Loop C partially closed (PDB 5AFM, Spurny et al., 2015). The amino acid sequences were aligned using ClustalW (http://www.ebi.ac.uk/Tools/msa/clustalw2/) and modeling was performed using MODELLER 9.19 (https://salilab.org/modeller/) (Sali et al., 1995). We tested the ligand docking in mouse α1/ε and α1/δ interfaces and in ten different subunit interfaces of the L-

AChR using the two different models for each interface. Ten models were generated for each interface, and the one with the lowest energy and the smallest percentage of amino acids in the disallowed region of the Ramachandran plot was selected for docking studies. ACh and bephenium were obtained from the PubChem database and docked separately using AUTODOCK 4.2 (Morris et al., 2009). A hundred genetic algorithm runs were performed for each condition. Clustering of the results was done with AUTODOCK based on a root-mean-square deviation cut-off of 2.0 Å. To evaluate the capability of each interface to bind agonist, we compared the best binding energy (BBE) and the frequency of conformations that bind the agonist in the correct orientation in the binding pocket. Docking results were corroborated in two different procedures and the most representative docking result was plotted with Discovery Studio Visualizer 4.5 (Dassault Systèmes BIOVIA, San Diego, 2016).

Statistics.

Experimental data are shown as mean ±S.D. Statistical comparisons were done using the Student's t test or one-way ANOVA with Bonferroni's multiple comparison post test. A level of $p<0.05$ was considered statistically significant.

Molecular Pharmacology Fast Forward. Published on September 6, 2018 as DOI: 10.1124/mol.118.113357
This article has not been copyedited and formatted. The final version may differ from this version.

Results

1-Behavioral effects of Bephenium on C. elegans.

To test if the anthelmintic drug bephenium is active on *C. elegans*, we synchronized populations of wild-type worms (N2 strain), exposed them to bephenium on agar plates, and measured the fraction of moving animals. We found that the exposure to bephenium produced spastic paralysis. The decrease in the percentage of moving animals as a function of drug concentration revealed an IC_{50} value of 2.2 mM when animals were pre-exposed for 1 h to bephenium at each tested concentration (Fig. 1A). As expected, identical behavior was observed in the PD4251 strain, which expresses GFP in muscle, and it was therefore used as a control strain for many assays.

Since one of the main targets of antiparasitic drugs is the levamisole-sensitive nAChR (L-AChR), we tested the action of bephenium on the strain *unc-38(e264)I* that lacks the UNC-38 subunit, which is an essential component of L-AChR (Fleming et al., 1997; Richmond and Jorgensen, 1999; Culetto et al., 2004). On this strain, 3 mM bephenium paralyzed 3.00 ± 2.70% and 9.71 ± 3.95% of animals after 1 and 2 h exposure, respectively. In contrast, for the PD4251 strain that contains wild-type L-AChRs, the percentage of paralyzed animals was 59.57 ± 6.08% and 74.86 ± 7.17%, respectively (n>25 worms per dish, n=7 dishes per condition) (Fig. 1B). The resistance to bephenium of worms lacking functional L-AChRs indicates that this receptor is a key target involved in its paralyzing activity.

It has been proposed that in *Haemonchus contortus* the nicotinic subunit ACR-8 is key for bephenium sensitivity (Charvet et al., 2012). ACR-8 is present in *C. elegans* muscle as a spare subunit and it may replace LEV-8 in its absence (Hernando et al., 2012). We therefore determined the action of bephenium in the *lev-8(x15)* strain that lacks the LEV-8 subunit and may contain ACR-8 in the pentameric L-AChR arrangement (Hernando et al., 2012). Synchronized PD4251 (wild-type L-AChR) and mutant *lev-8(x15)* worms (L-AChR lacking LEV-8) were exposed to 1 mM bephenium on agar plates. Whereas 6.27 ± 4.67% and 8.65 ± 7.09% of mutant worms were paralyzed after 1 and 2 h, respectively, 16.49 ± 8.09% and 25.43 ± 15.98% of control worms containing wild-type L-AChRs were paralyzed at 1 and 2 h, respectively (n>30 worms in each assay, n=8 dishes per condition). At both hours of exposure, the percentage of paralyzed animals was statistically significantly different between control and mutant animals (p=0.008 and p=0.017 for 1 and 2 h,

Molecular Pharmacology Fast Forward. Published on September 6, 2018 as DOI: 10.1124/mol.118.113357
This article has not been copyedited and formatted. The final version may differ from this version.

respectively). Thus, the mutant strain is partially resistant to bephenium, as shown for levamisole (Hernando et al., 2012).

To determine how bephenium affects the paralyzing effect of levamisole, we performed paralysis assays in the presence of bephenium (1 mM) and levamisole (0.03 mM) after 1 h and 2 h exposure. These concentrations are close to the IC_{50} values for the paralyzing effect of each drug. We found that 79.69 ± 13.04% (1 h) and 90.93 ± 10.08% (2 h) of adult worms were paralyzed with the drug combination whereas 38.01 ± 9.75% (1 h) and 72.78 ± 10.98% (2 h) were paralyzed in the presence of levamisole and 29.73 ± 6.62% (1 h) and 54.33± 9.67% (2 h) in the presence of bephenium (Fig. 1C) (n=6 simultaneous assays for all conditions, with >30 worms per each dish). There were statistically significant differences in the percentage of paralyzed worms between the drug combination and each individual drug ($p<0.001$). The fact that the paralyzing effects of both drugs are quite additive suggests that they act at the same target, the L-AChR.

2-Bephenium activates L-AChRs from C. elegans L1 muscle cells.

To unequivocally determine the molecular target of bephenium, we performed single-channel recordings from cultured embryonic cells that differentiate *in vitro* to the Larval 1 (L1) stage (Christensen et al., 2002). We first used the PD4251 strain, which produces GFP in all body wall muscles and allows their easily identification in culture.

As shown in Fig. 2A, 50 µM bephenium elicits single-channel currents from cell-attached patches from L1 muscle cells. Channel openings were not detected under similar conditions in the absence of bephenium (n=6). Single-channel activity elicited by bephenium shows a homogenous population of opening events of 3.56±0.62 pA (n=20) (100 mV holding potential) that appear mainly as isolated events and less often in short activation episodes composed of two or more openings (bursts) and at a constant frequency throughout the recording (at least 10 min) (Fig. 2A).

The pattern of channel activity and the amplitude of the opening events resemble those of L-AChR (Rayes et al., 2007; Hernando et al., 2012). From this receptor, single-channel openings are readily detected in the presence of ACh (0.1-300 µM) or levamisole (0.1-100 µM) but not in its absence (Rayes et al., 2007; Hernando et al., 2012). At 50 µM ACh, channel activity appears as high-frequency opening events of similar amplitude as those activated by bephenium (3.92 ± 0.39 pA at 100 mV pipette potential, n=8, p=0.132).

Molecular Pharmacology Fast Forward. Published on September 6, 2018 as DOI: 10.1124/mol.118.113357
This article has not been copyedited and formatted. The final version may differ from this version.

As with bephenium, opening events occur mainly isolated or in short bursts (Fig. 2A) and activity remains constant at least during a 7-min recording (Hernando et al., 2012).

We recorded single-channel currents activated by ACh or bephenium at a range of holding potentials and constructed voltage-current relationships. The estimated single-channel conductance for bephenium was 34.8 ± 0.2 pS (Fig. 2B), similar to that determined for ACh (35.0±1.2 pS; Hernando et al., 2012), thus suggesting, once more, that channel activity elicited by bephenium arises from the L-AChR.

To unequivocally confirm this statement, we made single-channel recordings from L1 muscle cells obtained from the *unc-38(e264)I* strain that lacks the essential UNC-38 subunit. No single-channel activity was detected from L1 cells derived from this strain that lacks L-AChRs either in the presence of 50 μM ACh (Rayes et al., 2007) or 50 μM bephenium (n= 10). This result is in full agreement with the behavioral results indicating that the strain lacking L-AChR is resistant to bephenium. Thus, bephenium-elicited channel activity arises from L-AChR.

We also determined if L-AChRs lacking LEV-8, which may contain the ACR-8 subunit instead of LEV-8, are activatable by bephenium by performing single-channel recordings from the *lev-8*(*x15*) strain. Single L-AChR activity in the presence of 30 μM bephenium was readily detected (Fig. 2C). The mean open duration of bephenium-activated channels (0.36 ± 0.16 ms, n=3 patches) was not statistically significantly different from that recorded with ACh as an agonist (0.30 ± 0.07 ms, n=3, p=0.558, Hernando et al., 2012). Moreover, examination of the recordings showed that bephenium-activated openings appear clustered in long activation episodes, separated by prolonged closed times (Fig. 2C). This pattern of channel activity is similar to that described for ACh (Fig. 2C) and was shown to arise from increased desensitization of the L-AChR lacking LEV-8 (Hernando et al., 2012). Thus, bephenium is also capable of inducing desensitization of the L-AChR.

3-Characterization of bephenium as an agonist and open-channel blocker of L-AChR

To characterize the action of bephenium as an L-AChR agonist, we recorded single-channel currents at a range of concentration and compared to those elicited by ACh. The minimum bephenium concentration that allowed detection of opening events was 0.5 μM, which is in the same order as that for ACh (0.1-0.5 μM) (Rayes et al., 2007; Hernando et al., 2012). At a wide range of bephenium concentration (0.5-250 μM), channel activity appeared mainly

Molecular Pharmacology Fast Forward. Published on September 6, 2018 as DOI: 10.1124/mol.118.113357
This article has not been copyedited and formatted. The final version may differ from this version.

as isolated opening events (Fig. 3A). At 50 μM, open time distributions showed a main open component of 0.21 ± 0.04 ms (n= 6), which is similar to that of 50 μM ACh-elicited channels (0.25 ± 0.03 ms, n=3). As shown in Fig. 3A, the open duration decreases as a function of bephenium concentration, indicating additional open channel block mediated by the drug. The reduction in open channel lifetime is statistically significant at concentrations higher than 100 μM, as shown for ACh (Hernando et al., 2012).

The decrease in open duration at high concentrations indicates that bephenium also acts as an open channel blocker. To characterize this effect, we used the simplest linear scheme (Scheme 1),

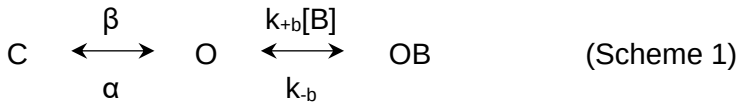

(Scheme 1)

In Scheme 1, C corresponds to closed, O to open and OB to blocked states. β and α are the opening and closing rates, respectively, and k_{+b} and k_{-b}, are the forward blocking and unblocking rates, respectively. From lineal regression analysis, we estimated the blocking constant from the slope of the relationship of the inverse of open channel lifetime, which is an approximation for α, and bephenium concentration (B in Scheme 1) (Fig. 3B). The estimated value, 2.1×10^7 $s^{-1}M^{-1}$, is similar to those reported for other open-channel blockers (Neher and Steinbach, 1978; Rayes et al., 2001).

Closed time histograms were fitted by two or more components. The main closed component corresponds to closing between isolated openings. This duration was 170.77 ± 66.68 ms (n=3) at 50 μM bephenium whereas it was 19.25 ± 8.53 ms at 50 μM ACh (n=3, and see Rayes et al., 2007).

4- L-AChR is the target of bephenium at L2 developmental stage.

We also evaluated whether bephenium recognizes a different target at a different developmental stage. To this end, we used another strategy that allows culture of L2 cells (Zhang et al., 2011). In the cultures, muscle cells are recognized by the typical morphology and have a greater size than those of L1 cultures (Zhang et al., 2011).

From these L2 cells, we detected for the first time single-channel activity elicited by ACh and compared to that elicited by bephenium. In general, the patterns of channel activity

Molecular Pharmacology Fast Forward. Published on September 6, 2018 as DOI: 10.1124/mol.118.113357
This article has not been copyedited and formatted. The final version may differ from this version.

elicited by ACh and bephenium were similar to those recorded from L1 cells, indicating that L-AChR is the main target for bephenium also in the L2 stage. Channel openings of a homogenous amplitude class were detected for both agonists, whose mean amplitudes at 100 mV were 3.20 ± 0.12 pA (n=4) and 3.36 ± 0.10 pA (n=3) for ACh (100 μM) and bephenium (50 μM). The mean open times were similar between bephenium and ACh: 0.16 ± 0.01 ms (n=4) and 0.18 ± 0.05 ms (n=4) for 100 μM ACh and 50 μM bephenium, respectively (p=0.63).

5-Bephenium is a weak agonist and a potent channel blocker of the mammalian muscle nAChR.

To determine if bephenium is selective for nematode nAChRs, we recorded single channels from cells expressing mammalian adult muscle nAChRs (Fig. 4). Bephenium elicited single nAChR currents at concentrations as low as 1 μM; under the same conditions channel openings were detected at 0.5 μM ACh. However, channel openings were markedly briefer than those activated by ACh. Open time distributions of 10 μM bephenium-activated channels were well fitted by a main component of 0.11 ± 0.05 ms (n=3) whereas the duration of the main open component was 1.22 ± 0.32 ms in the presence of 1-100 μM ACh (n=6 cells). At ACh concentrations higher than 10 μM, mammalian muscle nAChR opens typically in clusters of well-defined activation episodes (Bouzat et al., 2000; Bouzat and Sine, 2018) (Fig. 4A). Each activation episode begins with the transition of a single receptor from the desensitized to the activatable state and terminates by returning to the desensitized state. At 30 μM ACh, clusters of openings (mean cluster duration 144 ± 70 ms) showed intracluster closings whose mean duration was 1.80 ± 0.29 ms (n=6). In contrast, when nAChRs were activated by bephenium, even at concentrations as high as 300 μM, clusters were not distinguished (Fig. 4B). A similar behavior has been reported for other nAChR weak agonists (Akk and Steinbach, 2003). These results demonstrate that bephenium opens mammalian nAChR channels with greater latency than ACh, and once opened, channels close faster than in the presence of ACh, thus indicating that it is a weak agonist of mammalian nAChRs. In addition, the decrease of open channel duration as a function of bephenium concentration indicates that it also acts as an open channel blocker of the mammalian muscle nAChR. The analysis based on Scheme 1 estimated k_b= 7.98x10^7 M^{-1}s^{-1} for the blocking process, which is four-fold higher than that at the L-AChR, indicating that it is a more potent channel blocker at the mammalian receptor.

Molecular Pharmacology Fast Forward. Published on September 6, 2018 as DOI: 10.1124/mol.118.113357
This article has not been copyedited and formatted. The final version may differ from this version.

To further explore the action of bephenium at mammalian muscle nAChRs, we analyzed its effect on nAChR activation by ACh at positive and negative pipette potentials. At +70 mV holding potential, the presence of 30 μM bephenium produced important changes in the activity pattern elicited by 30 μM ACh (Fig. 4C). Openings were statistically significantly briefer: the duration of the main open component was reduced from ~1 ms to 0.36 ± 0.01 ms (n=3). Clusters appeared remarkably different in the presence of bephenium (Fig. 4C). Whereas in the presence of 30 μM ACh the duration of the main closed component was between 1 and 2 ms, an additional and novel major slower component of 17.9 ± 4.9 ms was detected with the drug combination (n=3). To determine if the effect of bephenium on ACh-channel activity was due to binding site competition or to channel block, we analyzed the changes at a negative holding potential (-70 mV). The rationale for this study is based on the fact that channel block could be different at the different membrane potentials because bephenium is positively charged whereas competition for the extracellular agonist binding site is less voltage dependent. At -70 mV pipette potential, nAChR activated by 30 μM ACh appeared in clear clusters, with a mean closed component of 2.60 ± 0.64 ms and a mean open component of 0.14 ± 0.04 ms (n=3). This type of activity did not differ significantly from that recorded with the combination of ACh and 30 μM bephenium at the same potential (Fig. 4C). In these recordings, clusters were clearly distinguished, and the mean durations of the main open and closed components were 0.17 ± 0.02 ms and 2.49 ± 0.19 ms, respectively. Increasing bephenium concentration to 100 μM in the presence of 30 μM ACh did not affect remarkably the mean duration of the main closed component at the negative pipette potential (3.0 ± 0.11 ms) but significantly enhanced it at +70 mV (46 ± 11 ms, n=3) when compared to ACh alone.

These results indicate that in the presence of ACh, bephenium acts mainly as a channel blocker at positive holding potentials. Moreover, the fact that it does not affect significantly the duration of closings of ACh-activated channels at negative holding potentials indicates that it cannot compete with ACh and it is therefore a low-affinity agonist.

To further confirm the weak activation, we recorded macroscopic currents elicited by bephenium (10-1000 μM) at 50 and -50 mV holding potentials. We found that at both potentials the maximal peak current for bephenium was lower than 2% of that elicited by a saturating ACh concentration (n=6), and in many cases was indistinguishable from the background noise. Thus, bephenium activates mammalian nAChRs very weakly.

6-Bephenium docks into the ACh binding site

Molecular Pharmacology Fast Forward. Published on September 6, 2018 as DOI: 10.1124/mol.118.113357
This article has not been copyedited and formatted. The final version may differ from this version.

To gain insights into how bephenium may activate nAChR by binding to the orthosteric agonist binding site we performed molecular docking studies. We made homology models of the extracellular domain of two adjacent subunits to form functional agonist binding sites based on two different crystal models that contain Loop C of the principal face of the binding site in different conformations. Loop C has been shown to be essential for triggering channel activation and moves from an open to a closed conformation after agonist binding (Billen et al., 2012). We used the α4β2 structure crystalized with nicotine that contains Loop C closed (PDB 5KXI) and the chimera α7/AChBP crystalized with the partial agonist lobeline that contains Loop C partially closed (PDB 5AFM). The disposition of the five L-AChR subunits in the pentamer as well as the number of functional binding sites remain unknown. We therefore modelled ten possible subunit interfaces of *C. elegans* L-AChR: UNC-63/UNC-29, UNC-38/UNC-29, LEV-8/LEV-1, LEV-8/UNC-63, LEV-8/UNC-38, LEV-8/UNC-29, UNC-63/UNC-38, UNC-38/UNC-63, UNC-63/LEV-1 and UNC-38/LEV-1 (the latter four only for the model with Loop C partially closed), and the two muscle subunit interfaces that comprise the agonist binding sites (α1/δ and α1/ε). For ACh, the conformations considered as favorable were those showing the previously described cation-π interactions between the amino group of the ligand and aromatic residues of the binding pocket (W55, Y93, W149, Y190, Y198, numbering corresponds to α1 subunit) (Dougherty 2007).

With the PDB 5KXI model, in all mammalian and nematode interfaces, ACh docking resulted in a main energetically favorable model with ACh oriented with its quaternary amine toward the membrane side or lower part of the cleft, similarly to carbamylcholine in AChBP (Celie et al., 2004). The positively charged group showed the potential to form the typical cation-π interaction with the indol group of W149 in Loop B. There is also the potential of ACh to form additional H-bonds with different residues of the complementary face. In all tested interfaces, the frequency of active conformations was higher than 40% (from 40 to 100%) and the BBE of ACh was similar among all tested interfaces (-4.3 to -5.1 Kcal/mol, Celie et al., 2004). Bephenium also docked into all interfaces, suggesting that it can activate nAChR through the orthosteric agonist binding site but there were important differences with ACh docking. Although bephenium has a quaternary ammonium group it was unable to make the typical cation-π interaction with W149 or with other aromatic groups at the cavity of all tested interfaces (Fig. 5A,C). Another difference with ACh was a higher heterogeneity of conformations, suggesting that it can adopt different conformations at the binding site as reported for some partial agonists (Hibbs et al., 2009). Instead of cation-π, bephenium

Molecular Pharmacology Fast Forward. Published on September 6, 2018 as DOI: 10.1124/mol.118.113357
This article has not been copyedited and formatted. The final version may differ from this version.

showed π-π interactions between one of its aromatic group and aromatic groups of residues Y93, W149, Y190, Y198 and W55 (Fig. 5A,C). It also showed the potential to form H-bonds, and other types of bonds, such as π-alkyl, with residues of the complementary face. Other interesting interactions were π-sulfur with the conserved cysteines (C192 and C193). The BBE was more negative for bephenium than ACh at all interfaces, ranging from -6.7 in LEV-8/UNC-63 to -8.7 Kcal/ mol in α1/δ. The comparison between mammalian and worm interfaces did not show important differences in the orientations of bephenium at the binding site (Fig. 5A,C).

Since partial agonists produce a partial contraction of Loop C around the binding site (Billen et al., 2012), we explored homology models in this conformation (Fig. 5B,D). Bephenium docked into the binding sites of all interfaces. All conformations showed similar BBE to those of 5KXI models (-8 to -6 Kcal/ mol). Importantly, in these models bephenium showed the potential to make the typical cation-π interactions with W149 and/or Y198 (Fig. 5B,D). The frequency of conformations with cation-π interactions in all worm interfaces was lower than 10% except for LEV-8/UNC-38 interface. Interestingly, in the LEV-8/UNC-38 interface, 80% of the conformations showed cation-π interactions, indicating that it may be an activatable site for bephenium. For the muscle nAChR, the typical cation-π interaction was observed in the α1/ε interface (about 18% frequency) but not in the α1/δ interface, suggesting that only one of the two sites could be activated by bephenium, which may explain the partial agonism.

Molecular Pharmacology Fast Forward. Published on September 6, 2018 as DOI: 10.1124/mol.118.113357
This article has not been copyedited and formatted. The final version may differ from this version.

Discussion

Parasitic nematodes negatively impact human and animal health. It has been estimated that as many as one-third of the world's population harbors a helminth infection. Due to the limited number of drugs available, there is an urgent need for concerted efforts on this area of research. Muscle nAChRs mediate body muscle contraction during locomotion in nematodes and are important targets of anthelmintic drugs (Jones et al., 2007). Despite the differences in subunit composition and pharmacology of muscle nAChRs among different parasites as well as between parasites and *C. elegans*, *C. elegans* has provided a means to decipher L-AChR subunit composition in parasites and has become an important model organism in the study of antiparasitic drugs (Brown et al., 2006; Neveu et al., 2010). Thus, the molecular characterization of *C. elegans* nAChRs is useful for highlighting similarities with parasite nAChRs and for providing information for recapitulating parasite nAChRs in *C. elegans* (Blanchard et al., 2018).

Whereas *C. elegans* nAChRs have been pharmacologically classified into nicotine- and levamisole-sensitive receptors, a wider spectrum of pharmacological classes has been reported for parasite nAChRs. Bephenium sensitive receptors are included as an additional nAChR class. Nevertheless, the molecular actions of bephenium on *C. elegans* have not been explored to date.

The analysis of single L-AChR channel properties from *C. elegans* mutants has indicated that five different subunits (UNC-63, UNC-38, UNC-29, LEV-1, and LEV-8) assemble into a main functional form of L-AChR (Rayes et al., 2007; Hernando et al., 2012). The lack of the non-essential subunits LEV-1 or LEV-8 leads to functional L-AChRs with different channel properties (Hernando et al., 2012). Thus, in wild-type muscle the assembly of the five subunits appears to be constrained but in the absence of non-essential subunits different pentameric arrangements occur. In parasites, the assembly appears to be not so strict since the orthologous subunits, such as UNC-29 and UNC-38, can combine into pentamers with different stoichiometries, thus resulting in a broader spectrum of pharmacological classes (Williamson et al., 2009). Sensitivity to bephenium has been attributed to Asu-UNC-63 subunit in *A. suum* (Williamson et al., 2009) or to ACR-8 subunit in *H. contortus* (Boulin et al., 2011; Charvet et al., 2012).

We here demonstrated that UNC-38 null mutants are resistant to the bephenium-paralyzing effect and lack single-channel activity elicited by this drug, thus indicating that L-AChR is the target for bephenium. We also demonstrated that in the L2 stage single-channel

Molecular Pharmacology Fast Forward. Published on September 6, 2018 as DOI: 10.1124/mol.118.113357
This article has not been copyedited and formatted. The final version may differ from this version.

activity of L-AChR elicited by ACh is similar to that in L1 and that L-AChR is also the target of bephenium at this developmental stage.

We showed that bephenium and levamisole have additive paralyzing effects and the combination of the two drugs has significantly higher efficacy, which is of importance since drug combinatorial therapies are convenient strategies to overcome the increasing resistance of parasites.

L-AChR activation is elicited by low concentrations of bephenium. The channel activity pattern as well as the mean duration of openings at concentrations below the blocking ones are identical to those determined in the presence of ACh, in contrast to the markedly differences between ACh and bephenium actions in the mammalian muscle nAChR. The only difference between ACh- and bephenium-elicited L-AChR channel activity is that the mean duration of the main closed component is systematically more prolonged with bephenium. Closed times from patches in which either the number of channels is not known or episodes of a single receptor molecule (clusters) cannot be distinguished do not provide relevant kinetic information (Bouzat and Mukhtasimova, 2018; Bouzat and Sine, 2018). However, the duration of the main closed component of recordings of ACh-activated L-AChR channels is relatively constant among patches and is dependent on agonist concentration (Rayes et al., 2007). Thus, we can speculate that the prolonged closed durations in the presence of bephenium with respect to equal concentrations of ACh may arise from a lower efficacy and/or slow channel block.

Because ACR-8 was proposed to be required for bephenium action in *H. contortus* (Charvet et al., 2012) and for levamisole sensitivity in parasite nAChRs (Blanchard et al., 2018), we explored its action in a *C. elegans* mutant strain lacking LEV-8, which may be replaced by ACR-8 in L-AChR (Hernando et al., 2012, Blanchard et al., 2018). We found that the mutant L-AChR is also activatable by bephenium, suggesting that both LEV-8 and ACR-8 can mediate bephenium responses in *C. elegan*s. Moreover, bephenium is capable of inducing desensitization of the mutant L-AChR. This capability may act as a protection for avoiding sustained activation which leads to paralysis, thus explaining the partial resistance of the strain lacking LEV-8 to bephenium. *acr-8* orthologs are widely distributed in parasitic nematode genomes, in contrast to *lev-8* orthologues that are only present in a subset of parasitic species (Blanchard et al., 2018). Thus, *C. elegans* strains carrying parasite ACR-8 subunits could be useful models to explore the kinetics of bephenium-activated channels (Blanchard et al., 2018).

Molecular Pharmacology Fast Forward. Published on September 6, 2018 as DOI: 10.1124/mol.118.113357
This article has not been copyedited and formatted. The final version may differ from this version.

Our studies showed that bephenium activates mammalian muscle nAChRs by acting as a weak agonist and a potent channel blocker, thus acting mainly as an inhibitor of ACh-activated channels. The main features revealing its weak action at mammalian nAChRs are the lack of clusters of openings over a range of concentrations, which differs from the activation by ACh or full agonists (Akk and Steinback, 2003; Bouzat and Sine, 2018; Bouzat and Mukhtasimova, 2018), and 10-fold reduced open duration with respect to ACh-elicited channels. Moreover, if its activity had been tested only at the macroscopic level, its action as a partial agonist would have not been detected. Combined application of ACh and bephenium revealed that the main action of the antiparasitic drug is to inhibit ACh-activated channel activity by voltage-dependent channel block and that it is a low-affinity agonist since it does not affect ACh-activation at negative holding potentials (at which channel block is reduced).

Our molecular docking studies have provided insights into nAChR activation by bephenium binding to the orthosteric site. The ligand-binding cavities are located between subunit interfaces. The α-subunits provides the principal face of each agonist site that is formed by Loops A-C which contribute to a nest of aromatic residues (Y190, W149, Y198, Y93) that stabilizes the ammonium of the agonist through cation-π interactions and/or hydrogen bonding (Xiu et al., 2009). Loop C closes to cap the agonist, an event associated with the triggering of channel opening (Unwin and Fujiyoshi, 2012; Mukhtasimova et al., 2009). Loop C adopts an uncapped conformation in the absence of agonist or in the presence of antagonists (Miller and Smart, 2009; Billen et al., 2012). X-ray structures of AChBP in complex with partial agonists showed an incomplete contraction of Loop C (Hibbs et al., 2009; Billen et al., 2012; Spurny et al., 2015). We therefore generated binding site interfaces on the basis of two structural models with Loop C both in a closed and in a partially closed conformations (as with partial agonists). In both models, bephenium docked into the binding site of all interfaces, indicating that it can act as an orthosteric agonist. For the model with Loop C closed the main features of bephenium binding were: i) the lack of cation-π interaction with W149 in Loop B that has been reported for most nAChR agonists (Billen et al., 2012; Post et al., 2017); ii) the potential to make π-π interactions between one of its aromatic groups and the aromatic groups of key tyrosine and tryptophan residues; and iii) the potential of novel π-sulfur interactions with the conserved cysteines at Loop C of the principal face. The results suggest new binding modes and explain the low efficacy by the lack of cation-π interactions. Alternatively, bephenium may cause an incomplete contraction of Loop C, which was evaluated in the second model. In these models, bephenium showed

Molecular Pharmacology Fast Forward. Published on September 6, 2018 as DOI: 10.1124/mol.118.113357
This article has not been copyedited and formatted. The final version may differ from this version.

the potential to form the typical cation-π interactions with W149 and/or Y198. The requirement of a partially closed Loop C to allow these key binding site interactions may explain the partial agonism. Although almost all worm interfaces also showed the capability to form cation-π interactions, the frequency was remarkably higher in the LEV-8/UNC-38 interface. This higher frequency and the possibility of multiple binding site interfaces may explain the higher efficacy of bephenium activation of the L-AChR compared to mammalian nAChRs. Unfortunately, the disposition of the subunits in the pentameric arrangement of L-AChR subunits remains unknown and, therefore, we cannot assure that this interface occurs in the native receptor. Remarkably, the α1/δ interface did not show cation-π interactions. Thus, the very weak action of bephenium for the mammalian nAChR may be explained by receptor activation from a single orthosteric binding site (α1/ε interface).

Our study provides novel insights into the molecular bases of anthelmintic drug action, which paves the way for the development of novel drugs.

Molecular Pharmacology Fast Forward. Published on September 6, 2018 as DOI: 10.1124/mol.118.113357
This article has not been copyedited and formatted. The final version may differ from this version.

Authorship Contributions

Participated in research design: Bouzat, Turani, Hernando, Corradi.

Conducted experiments: Turani, Hernando, Corradi.

Performed data analysis: Turani, Hernando, Corradi, Bouzat.

Wrote or contributed to the writing of the manuscript: Bouzat, Corradi, Turani.

Molecular Pharmacology Fast Forward. Published on September 6, 2018 as DOI: 10.1124/mol.118.113357
This article has not been copyedited and formatted. The final version may differ from this version.

REFERENCES

Akk G and Steinbach JH (2003) Activation and block of mouse muscle-type nicotinic receptors by tetraethylammonium. *J Physiol* **551**:155-68.

Billen B, Spurny R, Brams M, van Elk R, Valera-Kummer S, Yakel J L, Voets T, Bertrand D, Smit AB, and Ulens C (2012) Molecular actions of smoking cessation drugs at α4β2 nicotinic receptors defined in crystal structures of a homologous binding protein. *Proc Natl Acad Sci U S A* **109**:9173–9178.

Blanchard A, Guégnard F, Charvet CL, Crisford A, Courtot E, Sauvé C, Harmache A, Duguet T, O'Connor V, Castagnone-Sereno P, Reaves B, Wolstenholme AJ, Beech RN, Holden-Dye L, Neveu C (2018) Deciphering the molecular determinants of cholinergic anthelmintic sensitivity in nematodes: When novel functional validation approaches highlight major differences between the model *Caenorhabditis elegans* and parasitic species. *PLoS Pathog* **14**:e1006996. https://doi.org/10.1371/journal.ppat.1006996.

Boulin T, Gielen M, Richmond JE, Williams DC, Paoletti P, and Bessereau JL (2008) Eight genes are required for functional reconstitution of the *Caenorhabditis elegans* levamisole-sensitive acetylcholine receptor. *Proc Natl Acad Sci USA* **105:**18590–18595.

Boulin T, Fauvin A, Charvet CL, Cortet J, Cabaret J, Bessereau J-L and Neveu C (2011) Functional reconstitution of *Haemonchus contortus* acetylcholine receptors in *Xenopus* oocytes provides mechanistic insights into levamisole resistance. *Br J Pharmacol* **164:**1421–1432.

Bouzat C, Bren N, and Sine SM (1994) Structural basis of the different gating kinetics of fetal and adult nicotinic acetylcholine receptor. *Neuron* **13:**1395–1402.

Bouzat C, Barrantes F, and Sine SM (2000) Nicotinic receptor fourth transmembrane domain: hydrogen bonding by conserved threonine contributes to channel gating kinetics. *J Gen Physiol* **115**:663–672.

Bouzat C and Sine SM (2018) Nicotinic acetylcholine receptors at the single-channel level. *Br J Pharmacol* **175**:1789-1804.

Bouzat C and Mukhtasimova N (2018) The nicotinic acetylcholine receptor as a molecular machine for neuromuscular transmission. *Curr Opin Physiol* **4**:40-48.

Brown LA, Jones AK, Buckingham SD, Mee CJ, and Sattelle DB (2006) Contributions from *Caenorhabditis elegans* functional genetics to antiparasitic drug target identification and validation: nicotinic acetylcholine receptors, a case study. *Int J Parasitol* **36**:617– 624.

Burrows RB (1958) The anthelmintic effect of bephenium on *Ancylostoma caninum*. *J Parasitol* **44**:607–610.

Buxton SK, Charvet CL, Neveu C, Cabaret J, Cortet J, Peineau N, Abongwa M, Courtot E, Robertson AP, Martin RJ (2014) Investigation of acetylcholine receptor diversity in a

nematode parasite leads to characterization of tribendimidine- and derquantel-sensitive nAChRs. *PLoS Pathog* **10(1)**:e1003870. doi: 10.1371/journal.ppat.1003870.

Cecchini M and Changeux JP (2015) The nicotinic acetylcholine receptor and its prokaryotic homologues: Structure, conformational transitions & allosteric modulation. *Neuropharmacology* **96**:137-49.

Celie PH, van Rossum-Fikkert SE, van Dijk WJ, Brejc K, Smit AB and Sixma TK (2004) Nicotine and carbamylcholine binding to nicotinic acetylcholine receptors as studied in AChBP crystal structures. *Neuron* **41**:907-914.

Charvet CL, Robertson AP, Cabaret J, Martin RJ and Neveu C (2012) Selective effect of the anthelmintic bephenium on *Haemonchus contortus* levamisole-sensitive acetylcholine receptors. *Invert Neurosci* **12**:43–51.

Christensen M, Estevez A, Yin X, Fox R, Morrison R, McDonnell M, Gleason C, Miller DM 3rd, and Strange K (2002) A primary culture system for functional analysis of *C. elegans* neurons and muscle cells. *Neuron* **33**:503–514.

Copp FC, Standen OD, Scarnell J, Rawes DA, and Burrows RB (1958) A new series of anthelmintics. *Nature* **181**:183.

Corradi J, Gumilar F, and Bouzat C (2009) Single-channel kinetic analysis for activation and desensitization of homomeric 5-HT(3)A receptors. *Biophys J* **97**:1335–1345.

Culetto E, Baylis HA, Richmond JE, Jones AK, Fleming JT, Squires MD, Lewis JA, and Sattelle DB (2004) The *Caenorhabditis elegans unc-63* gene encodes a levamisole-sensitive nicotinic acetylcholine receptor α subunit. *J Biol Chem* **279**:42476–42483.

Dougherty DA (2007) Cation-π Interactions Involving Aromatic Amino Acids. *J Nutr* **137**:1504–1508.

Duguet TB, Charvet CL, Forrester SG, Wever CM, Dent JA, Neveu C, and Beech RN (2016) Recent Duplication and Functional Divergence in Parasitic Nematode Levamisole-Sensitive Acetylcholine Receptors. *PLoS Negl Trop Dis* **10**(7):e0004826. doi: 10.1371/journal.pntd.0004826

Fleming JT, Squire MD, Barnes TM, Tornoe C, Matsuda K, Ahnn J, Fire A, Sulston JE, Barnard EA, Sattelle DB, et al. (1997) *Caenorhabditis elegans* levamisole resistance genes *lev-1*, *unc-29* and *unc-38* encode functional nicotinic acetylcholine receptor subunits. *J Neurosci* **17:**5843–5857.

Gumilar F, Arias HR, Spitzmaul G, and Bouzat C (2003) Molecular mechanisms of inhibition of nicotinic acetylcholine receptors by tricyclic antidepressants. *Neuropharmacology* **45**:964-976.

Hernando G, Bergé I, Rayes D, and Bouzat C (2012) Contribution of Subunits to *Caenorhabditis elegans* Levamisole-Sensitive Nicotinic Receptor Function. *Mol Pharmacol* **82**:550-560.

Hibbs RE, Sulzenbacher G, Shi J, Talley TT, Conrod S, Kem WR, Taylor P, Marchot P, and Bourne Y (2009) Structural determinants for interaction of partial agonists with acetylcholine binding protein and neuronal alpha7 nicotinic acetylcholine receptor. *EMBO J* **28**:3040 – 3051.

Holden-Dye L and Walker RJ (2007) Anthelmintic drugs. *WormBook*, ed. The *C. elegans* Research Community, WormBook, doi/10.1895/wormbook.1.143.1, http://www.wormbook.org.

Jones AK, Davis P, Hodgkin J and Sattelle DB (2007) The nicotinic acetylcholine receptor gene family of the nematode *Cenorhabditis elegans*: an update on nomenclature. *Invert Neurosci* **7**:129-131.

Jones AK and Sattelle DB (2008) The cys-loop ligand-gated ion channel gene superfamily of the nematode, *Caenorhabditis elegans. Invert Neurosci* **8**:41-47.

Kalamida D, Poulas K, Avramopoulou V, Fostieri E, Lagoumintzis G, Lazaridis K, Sideri A, Zouridakis M and Tzartis SJ (2007) Muscle and neuronal nicotinic acetylcholine receptors. Structure, function and pathogenicity. *FEBS J* **274**:3799-845.

Lewis JA, Wu CH, Berg H, and Levine JH (1980) The genetics of levamisole resistance in the nematode *Caenorhabditis elegans*. *Genetics* **95**:905-928.

Martin RJ, Robertson AP and Bjorn H (1997) Target sites of anthelmintics. *Parasitology* **114**:S111–S124.

Miller PS and Smart TG (2009) Binding, activation and modulation of Cys-loop receptors. *Trends Pharmacol Sci* **31**:161-174.

Mongan NP., Baylis HA., Adcock C., Smith GR., Sansom MS. and Sattelle DB (1998) An extensive and diverse gene family of nicotinic acetylcholine receptor alpha subunits in *Caenorhabditis elegans*. *Receptors Channels* **6**:213-28.

Morales-Perez CL, Noviello CM, and Hibbs RE (2016) X-ray structure of the human alpha 4 beta 2 nicotinic receptor. *Nature* **538**:411-415.

Morris GM, Huey R, Lindstrom W, Sanner MF, Belew RK, Goodsell DS and Olson AJ (2009) AutoDock4 and AutoDockTools4: Automated docking with selective receptor flexibility. *J Comput Chem* **30**:2785-2791.

Mukhtasimova N, Lee W-Y, Wang H-L, and Sine SM (2009) Detection and trapping of intermediate states priming nicotinic receptor channel gating. *Nature* **459**:451-454.

Neher E and Steinbach JH (1978) Local anaesthetics transiently block currents through single acetylcholine-receptor channels. *J Physiol* **277**:153-76.

Neveu C, Charvet CL, Fauvin A, Cortet J, Beech RN, and Cabaret J (2010) Genetic diversity of levamisole receptor subunits in parasitic nematode species and abbreviated transcripts associated with resistance. *Pharmacogenet Genomics* **20**:414-425.

Pear WS, Nolan GP, Scott ML and Baltimore D (1993) Production of high-titer helper-free retroviruses by transient transfection. *Proc Natl Acad Sci U S A* **90**:8392–8396.

Post MR, Tender GS, Lester HA and Dougherty DA (2017) Secondary ammonium agonists make dual cation-π interactions in α4β2 nicotinic receptors. *eNeuro* 4(2). pii: ENEURO.0032-17.2017. DOI:http://dx.doi.org/10.1523/ENEURO.0032-17.2017.

Qian H, Martin RJ. and Robertson AP (2006) Pharmacology on *N-, L-,* and *B*-subtypes of nematode nAChR resolved at the single-channel level in *Ascaris suum*. *FASEB J* **20**:2108-2116.

Rayes D, De Rosa MJ, Spitzmaul G and Bouzat C (2001) The anthelmintic pyrantel acts as a low efficacious agonist and an open-channel blocker of mammalian acetylcholine receptors. *Neuropharmacology* **41**:238-45.

Rayes D, Flamini M, Hernando G and Bouzat C (2007) Activation of Single Nicotinic Receptor Channels from *Caenorhabditis elegans* Muscle. *Mol Pharmacol* **71**:1407–1415.

Richmond JE and Jorgensen EM (1999) One GABA and two acetylcholine receptors function at the *C. elegans* neuromuscular junction. *Nat Neurosci* **2**:791-797.

Robertson AP, Clark CL, Burns TA, Thompson DP, Geary TG, Trailovic SM and Martin RJ (2002) Paraherquamide and 2-deoxyparaherquamide distinguish cholinergic receptor subtypes in *Ascaris* muscle. *J Pharmacol Exp Ther* **302**:853–860.

Sali A, Potterton L, Yuan F, van Vlijmen H, Karplus M (1995) Evaluation of comparative protein modeling by MODELLER. *Proteins* **23**:318-26.

Sine SM (2012) End-plate acetylcholine receptor: structure, mechanism, pharmacology, and disease. *Physiol Rev* **92**:1189-1234.

Spencer WC, McWhirter R, Miller T, Strasbourger P, Thompson O, Hillier LW, Waterston RH and Miller DM (2014) Isolation of Specific Neurons from *C. elegans* Larvae for Gene Expression Profiling. *PLoS ONE* 9(11): e112102. doi:10.1371/journal.pone.0112102.

Unwin N (2005) Refined structure of the nicotinic acetylcholine receptor at 4A resolution. *J Mol Biol* **346:**967–989.

Unwin N and Fujiyoshi Y (2012) Gating movement of acetylcholine receptor caught by plunge-freezing. *J Mol Biol* **422**:617–634.

Verma S., Kashyap SS, Robertson AP and Martin RJ (2017) Functional genomics in *Brugia malayi* reveal diverse muscle nAChRs and differences between cholinergic anthelmintics. *Proc Natl Acad Sci U S A* **114**:5539-5544.

Williamson SM, Robertson AP, Brown L, Williams T, Woods DJ, Martin RJ, Sattelle DB and Wolstenholme AJ (2009) The nicotinic acetylcholine receptors of the parasitic nematode *Ascaris suum*: formation of two distinct drug targets by varying the relative

expression levels of two subunits. *PLoS Pathog* **5**:e1000517. doi: 10.1371/journal.ppat.1000517.

Xiu X, Puskar NL, Shanata JA, Lester HA, and Dougherty DA (2009) Nicotine binding to brain receptors requires a strong cation-pi interaction. *Nature* **458**:534-537.

Young MD, Jeffery GM, Freed JE, and Morehouse WG (1958) Bephenium, a new drug active against human hookworm. *J Parasitol* **44**:611–612.

Zhang S, Banerjee D, and Kuhn JR (2011) Isolation and Culture of Larval Cells from *C. elegans*. *PLoS ONE* 6(4): e19505. doi:10.1371/journal.pone.0019505.

Zhang S and Kuhn JR (2012) Cell isolation and culture. *WormBook*, ed. The *C. elegans* Research Community, WormBook,doi/10.1895/wormbook.1.157.1, http://www.wormbook.org.

Molecular Pharmacology Fast Forward. Published on September 6, 2018 as DOI: 10.1124/mol.118.113357
This article has not been copyedited and formatted. The final version may differ from this version.

Footnotes

a) This work was supported by grants from Universidad Nacional del Sur (UNS); Agencia Nacional de Promoción Científica y Tecnológica (ANPCYT); Consejo Nacional de Investigaciones Científicas y Técnicas (CONICET) Argentina; and Bill and Melinda Gates Foundation (OPP1098404) to CB.

b) Cecilia Bouzat. INIBIBB. CONICET Bahía Blanca. Km 7. 8000 Bahía Blanca. Argentina. E-mail: inbouzat@criba.edu.ar

Molecular Pharmacology Fast Forward. Published on September 6, 2018 as DOI: 10.1124/mol.118.113357
This article has not been copyedited and formatted. The final version may differ from this version.

Figure Legends.

Figure 1. Paralyzing effects of bephenium on C. elegans.

Chemical structures of bephenium and levamisole are shown at the top of the figure.
Assays were carried out on agar plates with synchronized populations of *C. elegans* at 20-22 ^{o}C.

A) Dose-response curve for the paralyzing effect of bephenium (1 h exposure) on wild-type *C. elegans* (N2 strain). The percentage of paralyzed animals was related to the control condition in the absence of bephenium and in the presence of the corresponding amount of DMSO. Body paralysis was defined as the lack of complete body movement in response to prodding. Values are mean percentages ± SD.

B) Comparison of the percentage of paralyzed animals containing (wild-type) or lacking L-AChRs (*unc38(e264)I*) after exposure to 1 or 2 h to 3 mM bephenium. Values are mean percentages ± SD derived from seven dishes per condition.
*** Indicates statistically significative differences respect to the wild-type condition ($p<0.001$).

C) Percentage of paralyzed worms exposed for 1 or 2 h to 0.03 mM levamisole, 1 mM bephenium or the two drugs combined. Values are mean percentages ± SD derived from three simultaneous assays for all conditions and two complete experiments performed on separate days.
Statistically comparisons between conditions with drug combination and individual drugs (*** $p<0.001$, ** $p<0.01$ and *$p<0.05$).

Figure 2. Single-channel currents elicited by bephenium from cultured L1 muscle cells.

A) Traces of singe-channel activity in the presence of 50 μM ACh or bephenium from wild-type L1 muscle cells are shown at two different temporal scales. At the right, representative open and closed duration histograms are shown for each condition. Channel openings are shown as upward deflections. Pipette potential: 100 mV.

B) Traces of single-channel activity in the presence of 30 μM bephenium at the indicated holding potential are shown filtered at 9 kHz with channel openings as upward deflections. Middle: Corresponding amplitude histograms. Right: Current-voltage relationship. The

conductance was obtained by linear regression analysis. Each point corresponds to the mean ± SD of three different recordings at each condition.

C) Continuous recordings from muscle cells derived from the *lev-8(x15)* mutant strain at 50 µM ACh and 30 µM bephenium. Pipette potential: 100 mV. Filter 9kHz. Single-channel activity of L-AChRs lacking LEV-8 decreases markedly with time and occurs in clusters.

Figure 3. Activation of L-AChR as a function of bephenium concentration.

A) L-AChR channels were recorded from cultured muscle cells of PD4251 worms at different bephenium concentrations and are shown at different temporal scales. Filter: 9 kHz. Holding potential: 100 mV. Representative open duration histograms are shown. Channel openings are shown as upward deflections.

B) Relationship between the reciprocal of the mean open duration (s^{-1}) as a function of bephenium concentration. The slope of the curves fitted by linear regression estimates the value of the forward blocking constant. Each point corresponds to the mean ± SD of three different patches for each condition.

Figure 4. Activation of mammalian nAChR by bephenium.

Single-channel recordings from BOSC 293 cells transfected with mammalian α1, β, ε and δ subunit cDNAs.

A) Mammalian nAChR channels activated by 30 µM ACh or bephenium are shown at two different time scales. In the presence of ACh, clusters of channel activity can be clearly distinguished. A representative cluster is shown at the lower amplitude resolution. No clusters are distinguished in the presence of bephenium. At the right, representative open time histograms are shown for each condition. Holding potential: 70 mV. Channels are shown as upward deflections.

B) Mammalian nAChR channels activated by bephenium at different concentrations. No clusters are distinguished at any concentration. At the right, representative open time histograms are shown. Holding potential: 70 mV. Channels are shown as upward deflections.

Molecular Pharmacology Fast Forward. Published on September 6, 2018 as DOI: 10.1124/mol.118.113357
This article has not been copyedited and formatted. The final version may differ from this version.

C) Single channel currents in the presence of 30 μM ACh alone or together with 30 μM bephenium were recorded at a pipette potential of +70 mV (top) or -70 mV (bottom). Channel openings are shown as upward deflections at +70 mV and as downward deflections at -70 mV.

Figure 5. Molecular docking of bephenium into homology modelled binding site interfaces.

Homology models of the extracellular domain of two adjacent subunits were created using the structure of PDB 5KXI (Panels A and C, Loop C closed) and PDB 5AFM (Panels B and D, Loop C partially closed). Panels A and B correspond to the LEV-8/ UNC-38 interface and Panels C and D to α1/ε interface. Loops from the principal face are shown in green and from the complementary face in blue. Bephenium is shown in yellow. Cation-π interactions are shown in orange (left panels), π-π in pink, H-bonds in green, π-sulfur in red, π-alkyl in purple.

Molecular Pharmacology Fast Forward. Published on September 6, 2018 as DOI: 10.1124/mol.118.113357
This article has not been copyedited and formatted. The final version may differ from this version.

Figure 1.

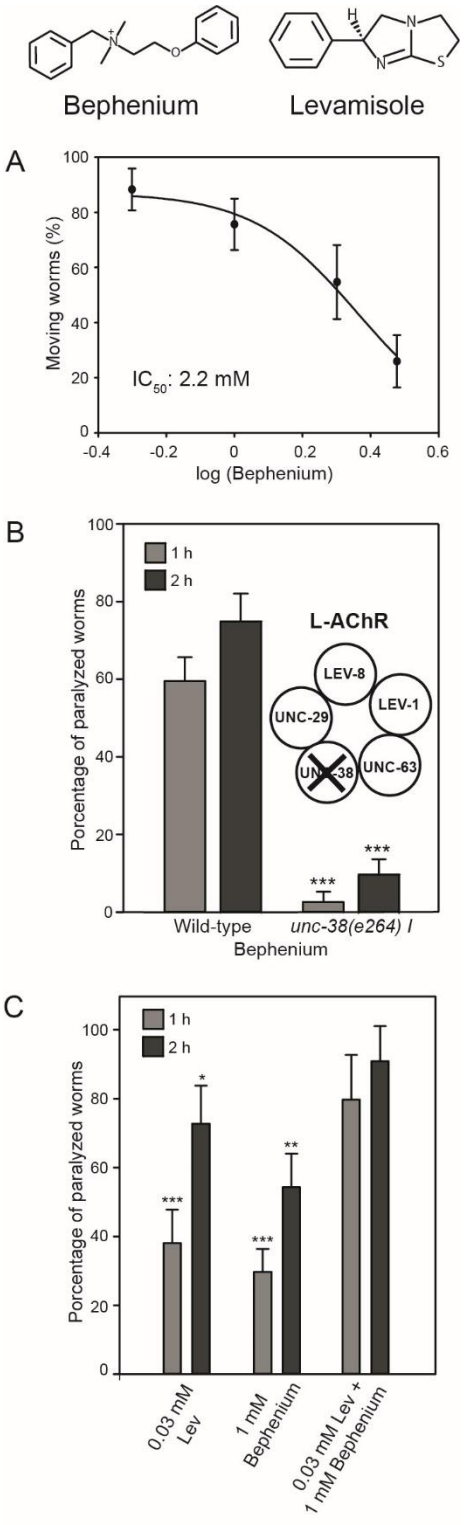

Molecular Pharmacology Fast Forward. Published on September 6, 2018 as DOI: 10.1124/mol.118.113357
This article has not been copyedited and formatted. The final version may differ from this version.

Figure 2.

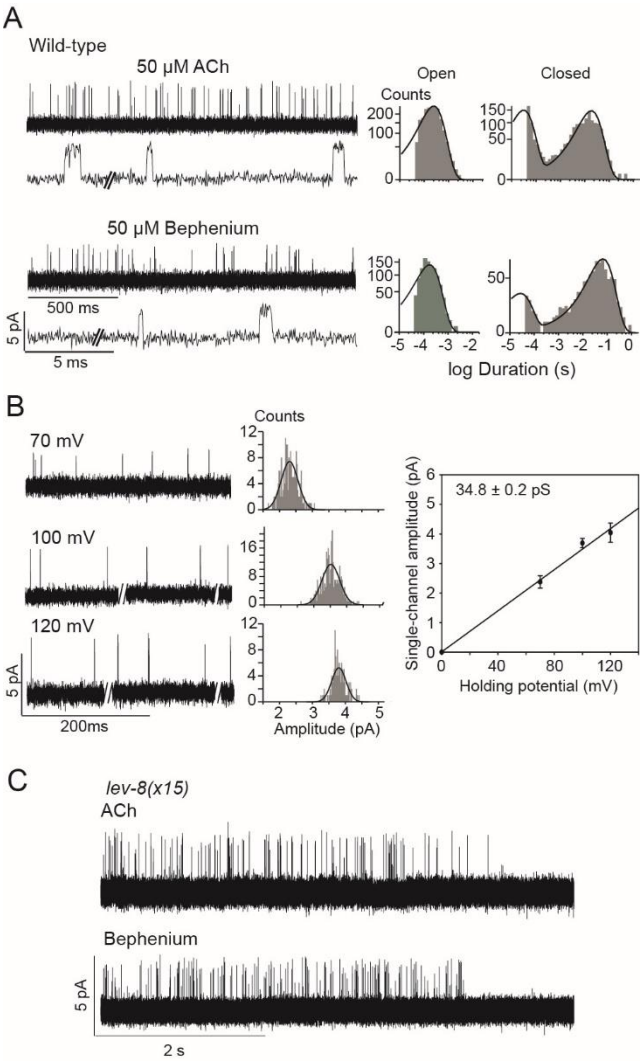

Molecular Pharmacology Fast Forward. Published on September 6, 2018 as DOI: 10.1124/mol.118.113357
This article has not been copyedited and formatted. The final version may differ from this version.

Figure 3.

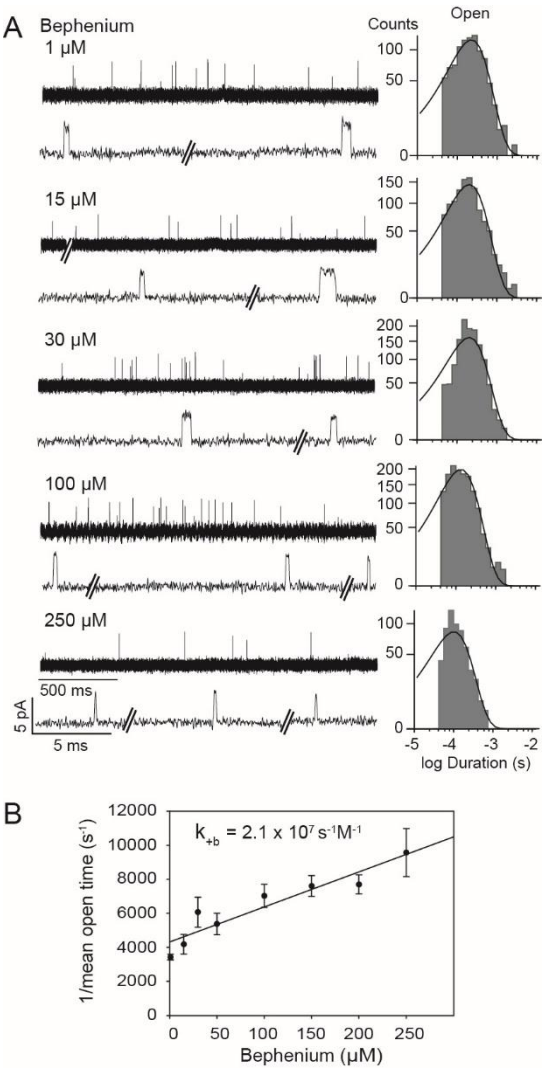

Molecular Pharmacology Fast Forward. Published on September 6, 2018 as DOI: 10.1124/mol.118.113357
This article has not been copyedited and formatted. The final version may differ from this version.

Figure 4.

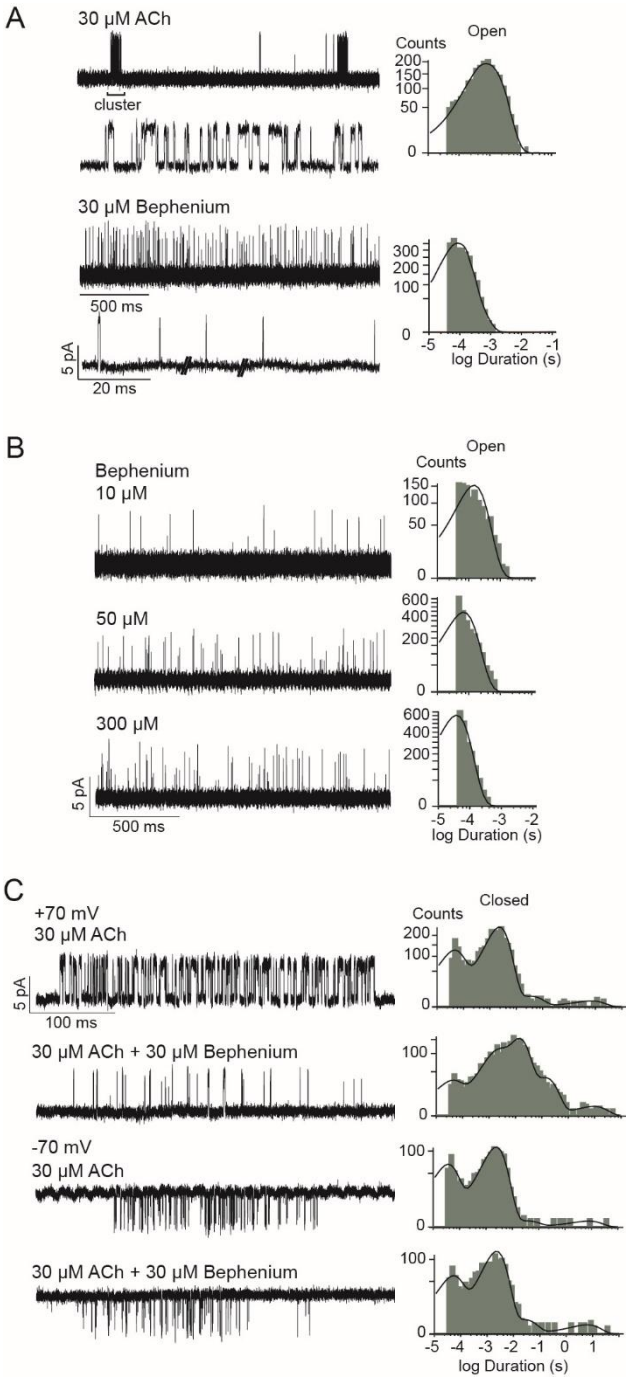

Molecular Pharmacology Fast Forward. Published on September 6, 2018 as DOI: 10.1124/mol.118.113357
This article has not been copyedited and formatted. The final version may differ from this version.

Figure 5.